Chapter 7

Nano- and Micro-Patterning of Gold Nanoparticles on PEG-Based Hydrogels for Controlling Cell Adhesion

Cigdem Yesildag, Zhenfang Zhang, Fang Ren, Gonzalo de Vicente and Marga C. Lensen

Additional information is available at the end of the chapter

http://dx.doi.org/10.5772/intechopen.71548

Abstract

Gold nanoparticles (Au NPs) have unique and tunable size- and shape-dependent optical and chemical properties and little toxicity. In this chapter, we describe results on Au NPs employed as cell-binding entities at biomaterials' interfaces. Hereby, Au NPs with different sizes and shapes were nano- or micro-patterned on the surface of poly(ethylene glycol) (PEG)-based hydrogels by using our recently developed patterning strategies based on soft lithography. These hybrid biomaterials can be applied in various biological or biomedical applications, such as for fundamental cell studies considering adhesion and migration, tissue engineering, drug delivery, or as biosensors by using surface plasmon resonance (SPR) or surface-enhanced Raman spectroscopy (SERS).

Keywords: gold nanoparticles, poly(ethylene glycol) hydrogels, biomaterials, nano- and micro-patterning, (wet) deprinting, cell adhesion

1. Introduction

In this chapter, an introduction to gold nanoparticles (Au NPs) and the applicability of them in biomaterials research as nanocomposites in combination with poly(ethylene glycol) (PEG)-based hydrogels, particularly for cell adhesion studies, will be introduced. First, Au NPs are described, with emphasis on their unique size- and shape-dependent properties; next, insight into the world of biomaterials is provided; lastly, our unique nano- and micro-patterning strategies of Au NPs on PEG-hydrogel surfaces will be explained, with the aim of controlling specific bio-interactions, for example, cell adhesion.

1.1. Gold nanoparticles

Colloidal gold particles have already been used in the seventeenth century because of their fascinating, different colors ranging from purple, green, blue to golden-yellow. They were mostly applied for decoration purposes of glass-ware or church windows. The first scientific literature on the field of gold colloids was published by Michael Faraday in June 1852, while he was studying light effects on thin gold films; he discovered nanometer-sized particles suspended in a solvent [1].

Since that time, a vast amount of research about colloidal and nanometer-sized gold nanoparticles (Au NPs) has been undertaken. Gold, as a noble metal, has great characteristics, such as chemical inertness, high stability, non-corrosive nature, and conductivity, which makes it a highly desired material in engineering, materials science, and catalysis. On top of that, Au NPs have unique size- and shape-dependent properties, which make this material even more interesting for nanoscience and nanotechnology, for example, in sensors, biomedical applications, catalysis, and optical technologies. While gold particles are chemically inert, they do have high binding affinity toward thiol groups or other sulfur-based entities, and also toward phosphoric or amino groups with less binding energy [2–4]. These properties allow the Au NPs to be easily functionalized with different desired molecules, which have the mentioned functional groups. In that way, Au NPs can be easily tuned for their specific application.

The size- and shape-dependent optical characteristics of Au NPs originate from localized surface plasmons [2, 3]. The surface plasmons are excited by the interaction of light (electromagnetic wave) with the electron clouds of the metallic particles (see **Figure 1**).

Au NPs exhibit localized surface plasmons, which are in the visible range of the electromagnetic spectrum. Different sizes or shapes of Au NPs make them appear in different colors to human eyes. The UV–Vis absorption wavelengths range from around 515 nm for the smallest Au NPs to higher wavelength with increasing sizes. Other shapes of Au NPs have different absorption bands in a UV–Vis spectrum. For example, rod-like Au NPs (Au nanorods) exhibit

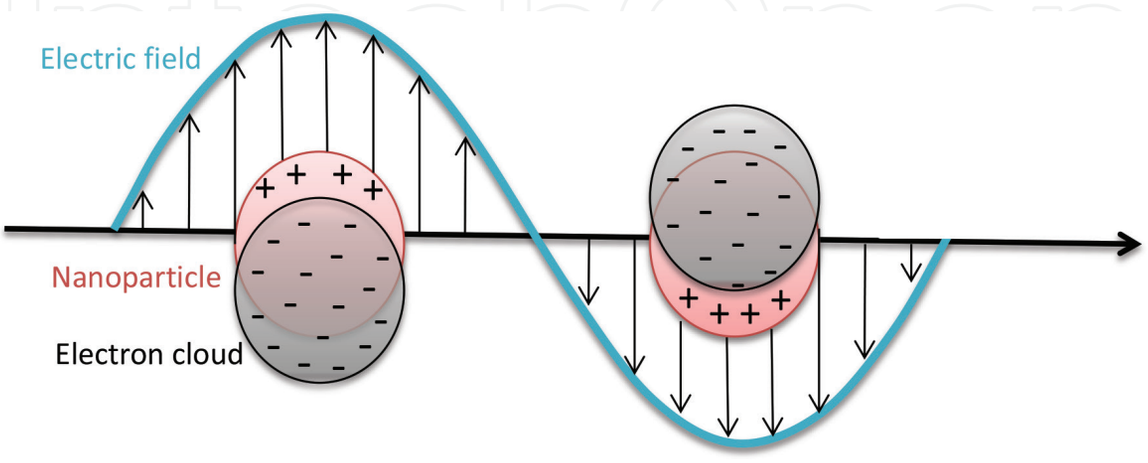

Figure 1. Surface plasmon effect of nanoparticles.

two absorption maxima. This occurs because of the correlation of the light or electromagnetic wave with the longitudinal part (longer part) of the particles and also with the transversal part (shorter part) of the Au nanorods, which appears as two different maxima in the same spectrum [5, 6]. Other shapes of Au NPs such as cubic, trihedral, decahedral, tetragonal, and so on, correlate according to the shape differently with the light, so each shape shows characteristic plasmon peaks in the UV–Vis spectra. In Section 2.1 (*vide infra*), a number of absorption spectra are depicted, corresponding to Au NPs that we synthesized with different sizes and shapes.

Au NPs have also the advantage that they are less toxic in comparison to other metallic particles. That is also why they can be applied in biological or biomedical applications [4]. We did discover recently, however, that some Au NPs with small sizes (e.g., 4.5 nm Au NPs spheres) or specific stabilizing agents, for example, cetyl trimethyl ammonium bromide (CTAB), do cause cytotoxic effects. Nevertheless, this makes them still applicable, for example, for selective killing of cancer cells [7, 8].

For biological systems, particles that exhibit surface plasmons in the IR range (around >700 nm) of the electromagnetic spectrum are highly desired, because in that region the biological tissues are transparent for this light and the light can go into deeper regions without hindrance, which is known as the optical biological window [9]. In this respect, rather large spherical Au NPs, for example, larger than 100 nm, or other shapes are interesting. Especially, Au nanorods are highly promising in this field because as mentioned before, they exhibit two localized plasmon stages: one in the wavelength at around 520 nm and the other one in the IR range depending on the length or aspect ratio of the particles. In that way, the Au NPs can be, for example, locally heated even above around 100°C by irradiation of the particles with IR-light source. This property of the Au NPs is used for photothermal therapy for killing unhealthy tissues and cancer cells. This is an alternative and less invasive cancer-healing method in comparison with the commonly used radiotherapy or chemotherapy [9]. Not only for photothermal therapy but also due to the high electron density of Au NPs, they are as useful as contrast agents for X-rays, magnetic resonance imaging (MRI), or other diagnostic devices. The optical properties of the Au NPs make them also useful for spectroscopic devices, especially for surface plasmon resonance spectroscopy (SPR) or surface-enhanced Raman spectroscopy (SERS). Based on these spectroscopic devices, many biosensor applications are conceivable [2].

Another promising application of Au NPs discussed in this chapter is in the area of fundamental cell adhesion studies. In our research, the respective Au NPs are patterned on bio-inert surfaces, namely on poly(ethylene glycol) (PEG)-based hydrogels (which will be further specified in the next section), and cell adhesion behavior of murine fibroblasts on the as-prepared nanocomposite biomaterial is investigated. The idea is that the specifically patterned Au NPs acted as anchor points for cell adhesion, and the particular micro- and nanoscale dimensions are investigated for their effectiveness to control cell behavior [10–12]. This goal is schematically depicted in **Figure 2**.

Such *in vitro* studies of fibroblast cell adhesion offer the possibility to get more insight into integration of implants or wound-healing processes and lead to develop novel biomaterials for applications in tissue engineering and regeneration. More information about biomaterials and an introduction into the basic phenomena at the bio-interfaces are given subsequently.

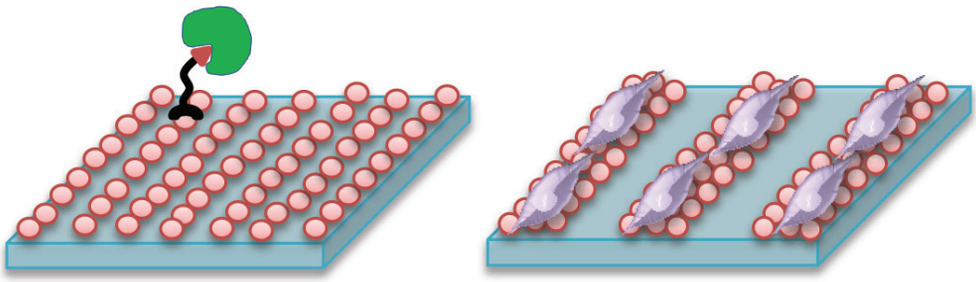

Figure 2. Nano- and micro-patterning of Au NPs on PEG-hydrogels for controlled binding of biomolecules and whole cells.

1.2. Biomaterials

In 1987, Williams defined biomaterials as "A biomaterial is a nonviable material used in a (medical) device, intended to interact with biological systems" [13]. Biomaterials are mainly used for implants [14, 15], prostheses [15], wound healing or tissue regeneration [16, 17], repairing or supporting materials [15, 18], and in biochips [19–21], which interact with biological fluids and can be used, for example, as biosensors [19, 21–24]. Biomaterials can be organic or inorganic in nature, for example, consisting of natural or synthetic polymers, metals, or ceramics, and may be composed of more than one type of nanomaterial or nanocomposite. Examples for polymeric biomaterials are hydrogels: hydrophilic polymeric networks which can adsorb huge amounts of water, without being dissolved and are similar to natural tissue scaffolds. That is why they are favorably used for biological tissue engineering, drug delivery, or cell biological research [25, 26]. In addition, combined hybrid or nanocomposite biomaterials, where the polymeric biomaterials are enriched with natural or inorganic nanoparticles, also offer novel, unique, and multifunctional properties for various biological applications.

Biomaterials contact and interact with biological systems at what is called the bio-interface [15, 27, 28]. Hence, there are several requirements for biomaterials not to elicit unwanted foreign body responses, such as inflammation reactions. The cyto-compatibility of biomaterials can be tested by several, standardized cytotoxicity tests. Also, the long-term stability or biodegradability may be important factors to consider. Before designing and fabricating new and improved biomaterials, the fundamental interactions at the bio-interface need to be understood. Therefore, it is important to realize that cell-substrate interactions are usually preceded by protein adsorption, which may be nonspecific, but could be predicted. Thus, controlling the initial protein adsorption is key to control specific bio-interaction, for example, cell adhesion.

Depending on the application, the interaction of cells with a biomaterial needs to be adherent or non-adherent. For example, biomaterials which are intended to be applied to interact with blood vessels, such as stents or artificial heart valves, should not be adhesive in order to avoid thrombosis effects [29]. Other biomaterials, which are designed for tissue regeneration, should enable specific cellular adhesion, guide constructive cellular migration, and

promote the proliferation and biosynthesis [30]. Protein adsorption and cell adhesion depend on (and thus can be controlled by) the chemical, physical, and mechanical properties of the bio-interface. These properties are the hydrophilicity, surface charges, anchored specific chemical functional groups or nanoparticles, surface roughness and porosity, nano- or micro-topography, and elasticity.

In order to enable the desired, specific bio-interaction, the nonspecific protein adsorption (NSPA) and unwanted cell adhesion should be suppressed. We have employed poly(ethylene glycol) (PEG)-based hydrogels as inert backgrounds onto which bioactive or adhesive cues (e.g., chemical, physical, or mechanical patterns), both at the micrometer and at the nanometer scale, are fabricated. PEG is a very popular biomaterial, due to its non-toxicity, non-fouling characteristics, and non-immunogenicity and has been widely used for drug delivery in medicine, in pharmacy, cell biological research, and in industry mainly as care products [31]. Nevertheless, even though PEG hydrogels are renowned for their intrinsically anti-adhesive properties toward proteins or cells, surface modifications such as nano- or micro-sized topography, gradient or patterned elasticity or chemical alterations do allow cell adhesion, as we and others have found [32–40].

The strategy to immobilize bio-functionalized Au NPs onto an inert PEG background to enable specific cell adhesion and prevent unwanted bio-interaction has proven to be very feasible and successful, as Spatz has demonstrated in several inspiring publications in the last two decades [41–45]. In his case, the Au NPs with controlled nanometer-sized distances were immobilized on PEG surfaces, bio-functionalized with cyclic RGD (a cell-adhesive peptide), and provided in that way integrin-mediated-binding sides for cell adhesion.

Notwithstanding the elegance and effectiveness of this strategy, we have discovered that the Au NPs do not even need to be specifically bio-functionalized in order to induce cell adhesion; we have observed unprecedented cell adhesion on nanocomposite bio-interfaces of PEG-based hydrogels with (citrate-stabilized) Au NPs [7, 10, 46]. The amount of cell adhesion was found to depend rationally on the density of the Au NPs at the bio-interface, indicating that the Au NPs are effective in enabling cell adhesion. Quite astonishingly, the number of adherent cells was observed to be even higher than on the positive control, tissue culture polystyrene (TCPS) surfaces [10]. We assume that the cell adhesion is promoted by the adsorption of adhesion-mediating proteins from the serum onto the Au NPs at the bio-interface. Besides tuning the density (and thus the average distance between Au NPs), we have strived to make controlled micro- and nano-patterns of Au NPs in order to elucidate which dimensions are critical in controlling cell adhesion and viability. For that, we have recently developed and reported about several novel patterning methodologies based on soft lithographic procedures. Both unpublished and published results will be discussed in the "Results and discussion" section.

1.3. Micro- and nano-patterning methods

Mimicking the characteristics of biological structures, especially micro- or nano-sized patterns of topography, elasticity or chemistry on biomaterials are highly desired in order to

first understand and then control the interaction of proteins, enzymes, or whole cells with bio-interfaces. There are several techniques to create patterned structures on surfaces which mostly rely on lithographic methods using irradiation or soft lithography. With some lithographic methods such as X-ray lithography or electron beam lithography, really small feature sizes of around 10 nm are accessible; if the irradiation energy is further increased, even sub-10-nm sizes can be achieved [47–49]. The drawback of these processes is that they require high-energy sources to modify very small areas during a long time period. By contrast, photolithography can be carried out using less expensive irradiation sources, but the resolution is inherently limited and the feature sizes are typically in the micrometer range. Scanning-probe-based-patterning techniques such as dip-pen lithography are promising methods to get sub-50-nm-sized structures without any irradiation source, but again this process is highly time consuming [50, 51].

Soft lithographic methods are versatile and attractive because of the following advantages: they are relatively cheap as they do not utilize high-energy irradiation sources, it is feasible to pattern large areas in a short period of time, and the processing is quite easy to handle. Micro-contact printing (μ-CP) is a widely used soft lithographic procedure, developed by Whitesides et al., where through stamping procedures with polydimethylsiloxane (PDMS) molecules or particles are transferred from the elastomeric stamp onto flat substrates [52, 53]. With this method, patterns of micrometer dimensions down to 250-nm sizes can be achieved.

In our lab, we have developed a very versatile soft lithographic method employing PEG-based hydrogel molds, which are filled by capillary action with another PEG-hydrogel precursor. With this method, called fill-molding in capillaries (FIMIC), we have successfully fabricated micro-patterns of elasticity and chemistry on PEG-based hydrogels, while the surface is topographically smooth [35, 54]. Those unique bio-interfaces are great platforms to control and study cellular behavior.

As far as nano-patterning is concerned, we have exploited Au NPs, which we either created on a hard substrate (e.g., glass or silicon wafer) by the so-called block copolymer micelle nanolithography method as developed by Glass et al. [41], or synthesized by wet chemistry and then immobilized on hard and soft surfaces (*vide infra*). In the former case, the characteristic, regular spacing between the Au NPs is determined by the length of the block copolymer chains. On top of that, Spatz et al. fabricated aperiodic micrometer-sized patterns by electron beam lithography, which is costly and slow.

We have taken a different approach to make micro-patterns of Au NPs, in that we have developed a micro-contact deprinting method (μ-CdP) where the Au NP-loaded block copolymer micelles were selectively peeled off from the hard substrate by a polystyrene (PS) stamp that was softened after annealing above its glass transition temperature [55]. With this soft lithographic approach, we were able to pattern large areas and even curved ones. Such hierarchical patterns can be transferred to soft hydrogel surfaces, for instance by nanomolding, using the Au NPs as templates to create nano-sized indents on PEG hydrogels [56]. By serendipity, we discovered that we could also transfer the whole pattern of Au NPs from the hard substrate to the soft hydrogel, namely by swelling the hydrogel replica before separating it from the mold. We observed selective cell adhesion to the micro-patterns of Au NPs, which we reasoned

could not be due to the tiny nano-topography. Atomic force microscopy (AFM) revealed that indeed the Au NPs had been transferred. Those yet unpublished results were the incentive of developing our wet micro-contact deprinting (wet μ-CdP) method, among others, which will be described in more detail in this chapter [12].

In addition, we have fabricated unique, hybrid hierarchical patterns, in which we "glued" micrometer-sized bars of PEG hydrogels onto the micro-patterns of Au NPs [57]. This was achieved by what we call "adhesive embossing," which is basically similar to the MIMIC method as developed by Whitesides [58, 59]. Starting from block copolymer micelles is, however, not always practical, since hard substrates are required. That is why, in the most recent years, we have synthesized Au NPs in solution, which can then be deposited on any substrate, including PDMS stamps and soft hydrogels. This advantage has enabled us to develop our own nano-contact printing (n-CP) strategies, for example, using wrinkled PDMS stamps that exhibit nanometer-sized grooves in which the Au NPs can be accumulated prior to the transfer to hydrogels [60, 61]. These results will also be highlighted in this chapter.

Another progress that we explain in the following is the use of multifunctional, reactive hydrogels that facilitate the transfer of Au NPs from hard substrate or stamps. We are currently perfecting such reactive μ-CP strategies and will report on the results soon. Very recently, we have already reported on the nano-contact transfer (n-CT) of Au NPs from silicon to multifunctional PEG hydrogels, in which the hydrogel films were functionalized with thiol-groups to bind strongly to the Au NPs [7, 10].

2. Experimental procedures

2.1. Preparation of Au NPs with different sizes and shapes

Differently sized spherical Au NPs ranging from around 20 nm to around 135 nm were achieved via the kinetically controlled seeding growth procedure according to Puntes et al. [62]. In the SEM images in **Figure 3(a)** and **(b)**, the sizes and structures of the synthesized smaller (20 nm) and larger (50 nm) spherical Au NPs are shown as representative examples. Below the SEM images in **Figure 3**, the respective UV–Vis spectra with the plasmon peaks at around 520–540 nm are shown. Hollow urchin-like particles (Au nanostars) were synthesized using the galvanic reduction effect of gold ions on the surface of sacrificial silver nanoparticles (Ag NPs seeds) [63]. The sizes of the Au nanostars varied between 50 and 150 nm (see **Figure 3(c)**. In some cases longer, rodlike Au nanostar shapes could also be observed, which might be caused by the agglomeration of Ag NP seeds before the addition of gold ions and which might be also the reason for larger-sized spherical particles. In the UV–Vis spectrum in **Figure 3(c)**, the plasmon peak is at 750 nm and also a shoulder peak at 600 nm is observed, which is probably due to the polydispersity of the particle sizes.

Au NPs with different shapes were synthesized by the polyol process [64]. Following this procedure, among others, cubic, tetrahedral, decahedral, icosahedral, trihedral, and platelet Au NPs shapes could be achieved. In **Figure 3(d)**, the SEM image and the UV–Vis spectrum

of decahedral Au NPs are shown as example. The sizes of the particles varied between 70 and 180 nm, and the absorption maximum is found around 590 nm. Au nanorods were synthesized using cetyl trimethyl ammonium bromide (CTAB) as stabilizing agent and 5-brome salicylic acid as structure-directing agent using the seed-mediated growth process [65]. In the SEM image in **Figure 3(e)**, the structure and the UV–Vis spectrum of the Au nanorods are shown: The lengths of the Au nanorods were around 50 nm and the widths were around 15 nm. Expectedly, there were two plasmon peaks which appeared due to the longitudinal and transversal interaction of the light with the Au nanorods.

2.2. Preparation of functional PEG hydrogels

In this study, PEG hydrogels were synthesized from different precursors, for example, linear or star-shaped PEG macromonomers, bearing specific chemical end groups. More specifically, linear PEG macromonomers with a molecular weight of 575 g/mol and eight-arm star-shaped PEG precursors (8PEG) with a molecular weight of ca. 15 kDa were used. PEG macromonomers with acrylate end groups were crosslinked via the UV-photo-crosslinking procedure with 1% of photo-initiator (Irgacure 2959), while 8PEG macromonomers with acrylate or vinyl sulfone end groups could be crosslinked with the addition of ammonia via Michael-type addition reactions as well [66]. Depending on the precursor type (molecular structure, weight, and crosslinking procedure), PEG hydrogels with different network structures and corresponding elastic properties were obtained. Hydrogels from linear PEG precursors with shorter chain length were quite stiff, exhibiting Young's elastic moduli of around 20 MPa in the swollen state, whereas hydrogels from 8PEG precursors were much softer with elasticity values of 0.27 MPa for swollen hydrogels [54, 67].

The great advantage of using 8PEG hydrogels is the fact that for crosslinking, only minimally two out of eight arms are required, and the other (up to six) arms can remain available for

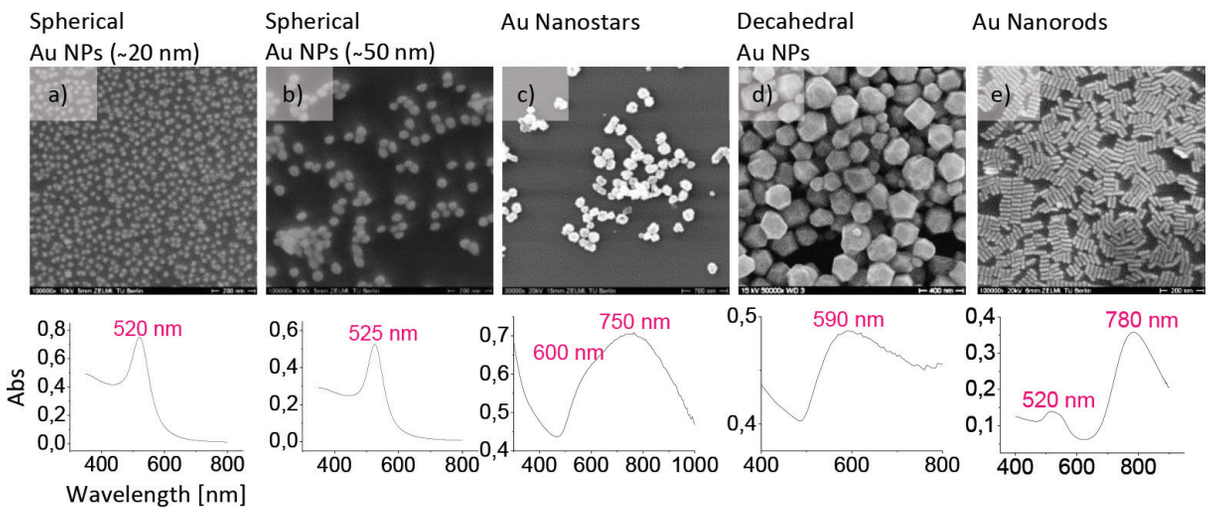

Figure 3. SEM images (top) and respective UV–Vis spectra (below) of Au NPs with different sizes and shapes: (a) smaller spheres ⟨ 20 nm); (b) larger spheres ⟨ 50 nm); (c) Au nanostars; (d) decahedral Au NPs; (e) Au nanorods. Scale bars: (a) 200 nm; (b) 200 nm; (c) 700 nm; (d) 400 nm; (e) 200 nm.

further chemical (multi-)functionalization with various end groups by clever tuning of the reaction conditions [10]. In this work, the incorporation of Au NPs was desired, so the functionalization of the hydrogels surfaces with thiol (SH)-molecules (dithiothreitol (DTT)) has been effectively employed in order to ensure strong chemical interactions between the Au NPs and the PEG hydrogels [10, 11].

2.3. Transfer of Au NPs onto PEG hydrogels

For the aim of obtaining soft, PEG-based hydrogel biomaterials with specific cell adhesion sites, Au NPs can be immobilized on PEG surfaces. Intuitively, one would expect that a covalent binding of the Au NPs with the gel is required, since the Au NPs might otherwise come loose in cell culture. Thus, it is sensible to functionalize the Au NPs with acrylate groups that will covalently link the Au NPs to the acrylate-functionalized PEG-hydrogel precursors, an approach that for instance Spatz' group has reported on. Nevertheless, as was already pointed out in Section 1.3., we have greatly simplified the mechanisms of transferring (patterned) Au NPs from hard substrates to soft, biomimetic hydrogels. For example, by virtue of swelling, no linker molecules are needed at all to transfer Au NPs from solid supports, for example, silicon wafers or glass, onto PEG-based hydrogels [12]. Interestingly, we have observed that the Au NPs are effectively embedded in the PEG hydrogel and do not escape from the bio-interface during cell culture.

Taking advantage of this simple and effective transfer mechanism, we have been able to transfer synthesized (citrate-stabilized) Au NPs from several, different substrates onto PEG hydrogels. Of particular interest is naturally the transfer of micro- or nano-patterns of Au NPs, which can be fabricated on hard substrates or stamps by the various patterning techniques that were introduced, that is, μ-CP and wet μ-CdP, and will be discussed in more detail in the next section.

In the simplest case, the surface of the solid support (glass, silicon wafer, or PDMS stamp) can be functionalized with amino-silane molecules, in order to have some, relatively weak binding of the negatively charged, citrate-stabilized Au NPs. On this Au NPs-coated layer, the acrylated PEG precursor with photo-initiator is added and the UV-photo-crosslinking procedure performed. Thereafter the hydrogel, which is still on the surface of the template with the Au NPs coating, is wetted by some drops of water. After the hydrogel has been fully hydrated, it is separated from the surface while peeling off the Au NPs from the solid support (see **Figure 4**).

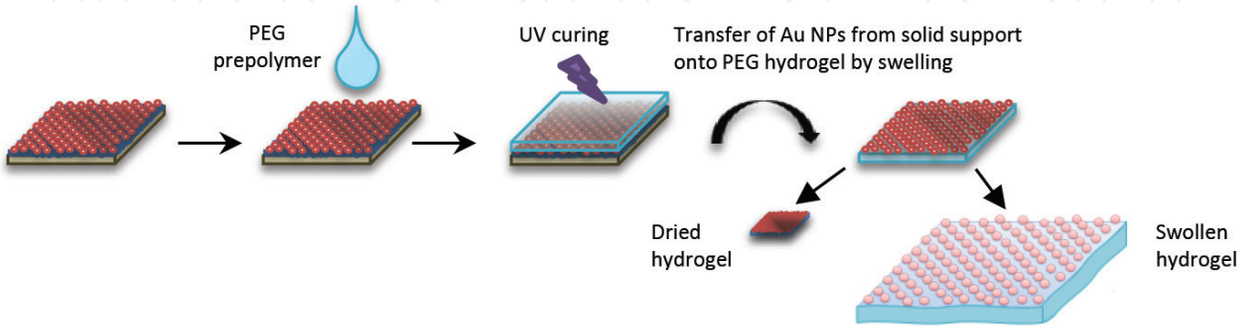

Figure 4. Scheme of transferring Au NPs from solid supports (e.g., silicon wafer or PDMS mold) onto PEG hydrogels by swelling of the hydrogel; size differences of the hydrogels in dry or swollen state. Image adapted from Yesildag et al. [12].

As an alternative to transferring Au NPs by virtue of the hydrogel's swelling property, we can employ (multi)functional or reactive PEG hydrogels to transfer whole (patterns of) Au NPs from a solid support or an elastomeric stamp. This strategy, which is schematically depicted in **Figure 5(a)**, also results in effective immobilization of Au NPs at the bio-interface, which has enabled us to study the effect of the Au NPs density on cell adhesion [10].

In this case, the physical and chemical properties of the hydrogel are of crucial importance for the transfer efficiency [10]. Non-functionalized and rigid hydrogels from linear PEG precursors need to be pressed onto the template in order to transfer maximally around 50–60% of Au NPs onto its surface [61], whereas multifunctional 8PEG hydrogels with thiol-surface functions are able to transfer the Au NPs quantitatively by mere conformal contact of the stand-alone hydrogel with the Au NPs-coated surface (see **Figure 5**).

2.4. Transferring patterns of Au NPs

After having introduced the basic transfer possibilities of the Au NPs from solid supports such as silicon wafers or PDMS molds onto PEG-based hydrogels, in the following, the transfer of micro- or nano-patterns of Au NPs will be discussed. In increasing order of complexity, these are (i) μ-CP of silane agents, (ii) wet micro-contact deprinting [12], and (iii) nano-contact transfer via wrinkled PDMS stamps [61].

2.4.1. Patterning of silane agents

In our experience, amino-silanization of silica-based substrates has proven to be effective in guiding the immobilization of citrate-stabilized Au NPs in a good, homogeneous fashion.

[12, 61]. This knowledge has been applied in fabricating micro-patterns of Au NPs on such substrates, for instance by applying μ-CP of different silanes (adhesive vs. repellent to our Au NPs). This procedure is schematically depicted in **Figure 6**.

In detail, first of all amino-silane molecules were printed on the surface of the silicon wafers using micro-relief-molded PDMS stamps [68]. The remaining, non-stamped areas were kept either non-functionalized or were backfilled with another type of silane, which has less attractive interactions with the Au NPs. While coating of a surface with amino-silanes causes highly

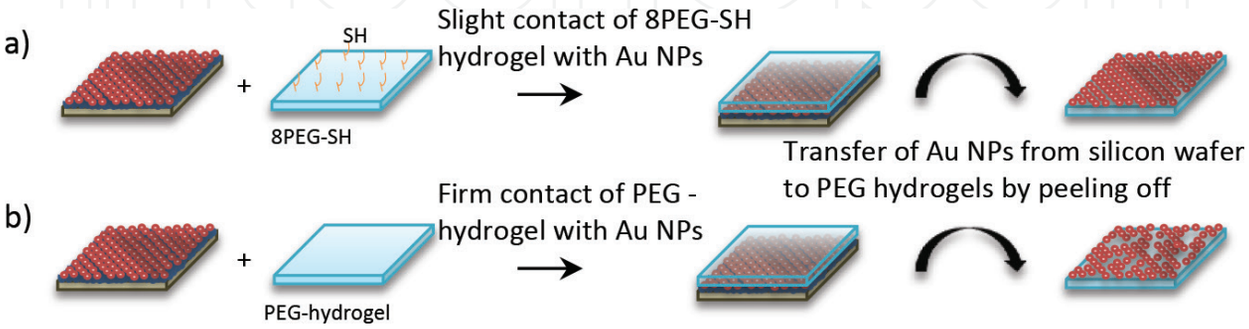

Figure 5. Scheme of transferring Au NPs from solid supports onto PEG hydrogels by contacting the hydrogel; (a) transfer to SH-functionalized 8PEG by slight contact; (b) transfer to non-functionalized linear PEG by firm contact.

http://dx.doi.org/10.5772/intechopen.71548

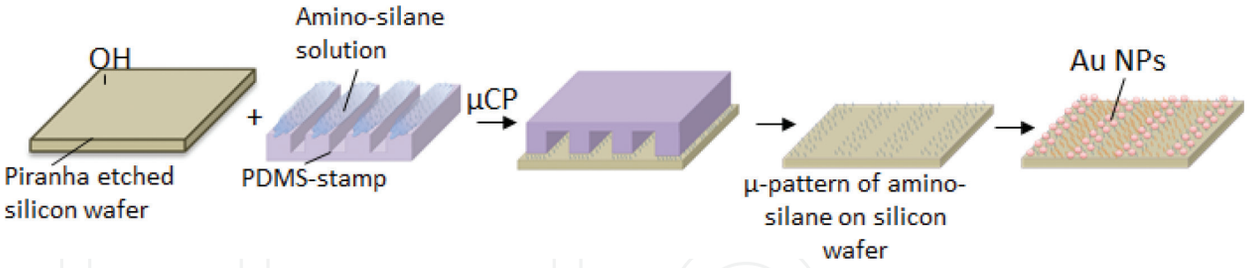

Figure 6. Schematic view of micro-patterning of silanes.

densely packed citrate-capped Au NPs [10, 11, 61] due to electrostatic interactions, backfilling of the remaining area with other silanes (e.g., with end groups: –OH, $–CH_3$, $–CF_3$) minimizes the adhesion of citrate-capped Au NPs. These Au NPs patterns were finally transferred onto PEG-hydrogel surfaces, for instance by virtue of swelling the UV-cured film before peeling it off (**Figure 7**).

As seen in the representative SEM image of the hydrogel after transfer (**Figure 8**), the Au NPs were more densely packed on amino-silane layers and more loosely packed on the other areas. While this procedure is somehow effective, the resolution and contrast of the pattern is not quite satisfactory. For achieving better-defined micro-patterns of Au NPs, we have developed novel patterning strategies, one of which is our recently invented wet µ-CdP method.

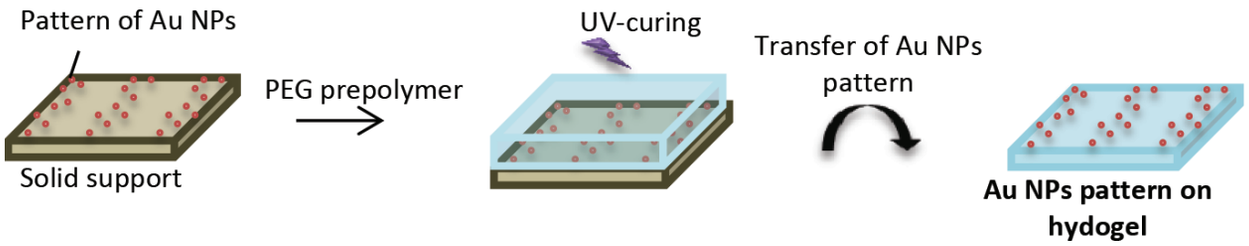

Figure 7. Schematic view of Au NPs pattern transfer from solid supports onto PEG hydrogels.

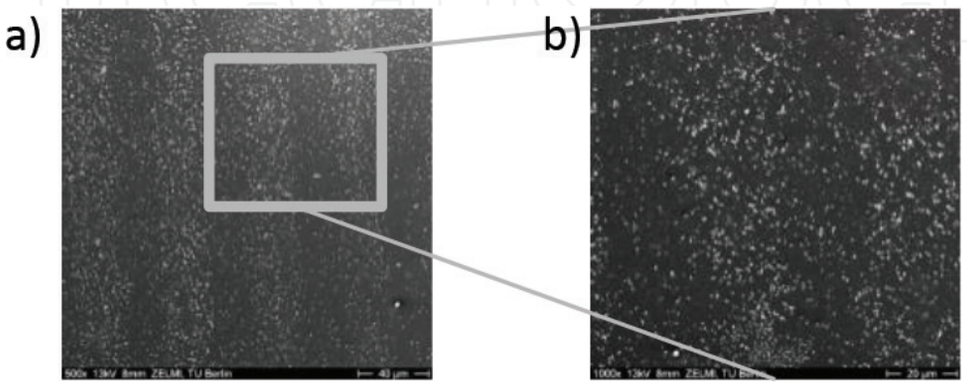

Figure 8. SEM image of Au NPs on PEG hydrogel via µ-CP of different silanes. Scale bars: (a) 40 µm; (b) 20 µm.

2.4.2. Wet micro-contact deprinting

The strategy for the wet micro-contact deprinting (wet μ-CdP) consists of removing Au NPs from defined regions of the silicon wafer by virtue of the swelling effect of the hydrogel. Using this method, well-defined micro-patterns of Au NPs lines (**Figure 9**) and rectangles (**Figure 10**) on solid supports such as silicon wafers can be created, as we recently reported [12]. Again, these resulting patterns could then be transferred from the hard substrate to the soft surface of PEG hydrogels.

In the wet μ-CdP procedure, the first challenge is to create a homogeneous monolayer of Au NPs on silicon wafers. As described earlier, the amino-silanization of silicon wafers has demonstrated to be effective to achieve a good surface coating on which the Au NPs are nicely immobilized. Next, in order to make patterns of the Au NPs, a PDMS mold with micro-sized relief line structures on its surface was placed on the Au NPs-decorated silicon wafer, creating line channels. Subsequently, by capillary action, the thus created channels were filled with the liquid PEG prepolymer and cured under UV light. After UV curing, the PDMS mold was removed, leaving an ordered pattern of PEG micro-stripes on the Au NPs-layered silicon wafer. This step, which we previously denoted "adhesive embossing" [57], is basically what Whitesides et al. coined MIMIC [58].

The novel aspect of the wet μ-CdP procedure is the last step, in which the cured PEG micro-stripes are removed by swelling in water. During the swelling, the Au NPs are taken away by the PEG hydrogel on the area where the stripes had been in contact with the Au NPs surface, while the non-contacted Au NPs are left as well-ordered micro-patterns of Au NPs on the surface of the silicon wafer [12].

In **Figure 11**, SEM images of resulting line patterns of Au NPs on silicon wafers are shown; here, the brighter lines are the Au NPs lines and the darker lines are empty areas on the silicon wafer, where the former Au NPs were deprinted by the PEG-hydrogel micro-stripes. The uptake of the Au NPs by the PEG hydrogel through swelling is so effective that no Au NPs were found on these areas. This method works with different types of Au NPs, for example, in **Figure 11(a)** spherical Au NPs and in (b) Au nanostars had been micro-patterned. Furthermore, using the wet μ-CdP process, rectangular patterns of Au NPs could be achieved as well via repeating the process with the PDMS mold oriented perpendicularly to the first pattern of micro-lines, which is shown in the SEM image in **Figure 11(c)**. In a further step,

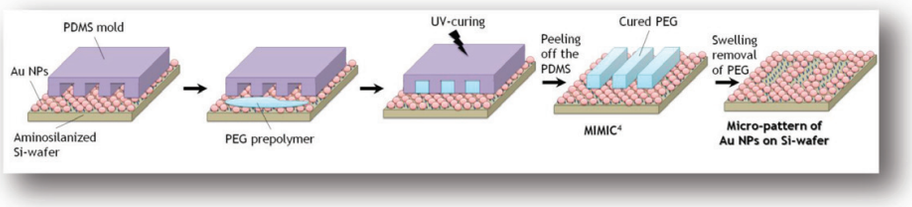

Figure 9. Schematic view of the wet micro-contact deprinting (wet μ-CdP) process for fabricating micrometer-sized line patterns [12].

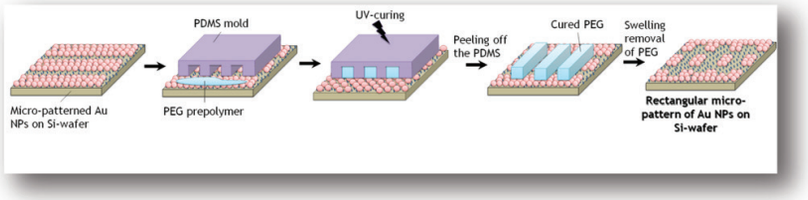

Figure 10. Schematic view of the wet micro-contact deprinting (wet μ-CdP) process for fabricating rectangular patterns [12].

again, the successful micro-patterns of Au NPs could be effectively transferred as a whole from the silicon wafer onto PEG hydrogels, for example, via the wet deprinting method, as illustrated in **Figure 7** (*vide supra*).

On the resulting micro-patterned PEG hydrogels, cell adhesion of murine fibroblasts (L929) was investigated. As can be seen in the optical images in **Figure 12**, fibroblast cells were clearly adhering and aligning only on the darker lines, which in this case correspond to the Au NPs patterns due to the optical contrast, while the non-functionalized PEG hydrogel appears as the brighter lines (see **Figure 12(a)**). Interestingly, in **Figure 12(b)**, the edge of the pattern lines, that is, where the original PDSM mold was not filled, and Au NPs were not removed in the wet μ-CdP process, can be recognized. Even more intriguingly, on this area, where the original, non-patterned layer of Au NPs has been transferred by wet deprinting, the cells were adhering and spreading in apparently random directions, whereas on the patterned lines, the cells were observed to align and elongate along the lines.

Cell adhesion of fibroblasts was also studied on the rectangular patterns of Au NPs on PEG hydrogel as fabricated by the wet μ-CdP method. The results are depicted in **Figure 13**. Similar to the case of the line patterns, it is evident that the fibroblasts preferentially adhere on the Au NPs-patterned areas, while the pure PEG areas are free of cells.

The pattern of the Au NPs rectangles in **Figure 13** had widths of 20 μm and lengths of 25 μm, which is comparable to usual fibroblast sizes of around 10–20 μm for round or little spread cells, so that on some rectangles, one or two cells were sitting next to each other. In a few cases,

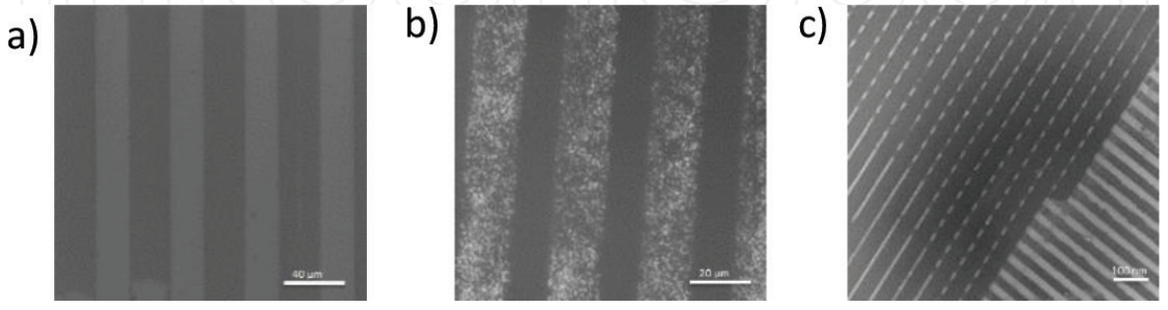

Figure 11. SEM images of Au NP (a–b) lines and (c) rectangular patterns of (a) spherical Au NPs (b) Au nanostars and (c) spherical Au NPs. Scale bars: (a) 40 μm; (b) 20 μm; (c) 100 nm. Image (c) modified from Yesildag et al. [12].

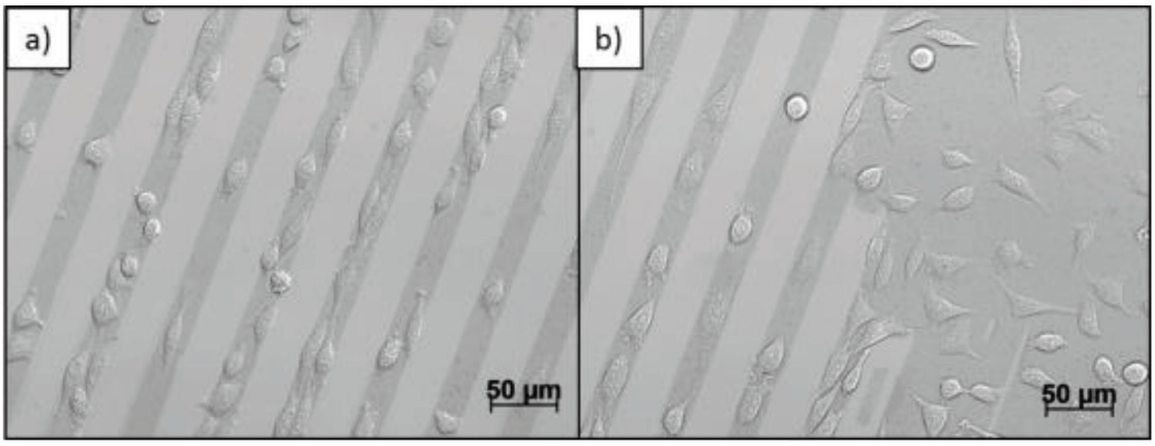

Figure 12. Optical image of fibroblast adhesion on Au NPs-patterned PEG hydrogel. The darker lines correspond to the patterns of Au NPs. Scale bars: 50 µm [12].

even three cells were accommodated in one rectangle of Au NPs. The distances among the rectangles were 10 µm on one side and 25 µm on the other side; on the area with a distance of 25 µm no cells were observable, whereas a separation of the rectangles of 10 µm allowed cells to have contacts with two parallel rectangles at the same time, so that the PEG area in the middle was bridged over by the cells, which can be observed in a few cases in **Figure 13**.

To round up this discussion of the wet µ-CdP results, by using this patterning method, very well-defined Au NPs patterns with line or rectangular shapes on PEG hydrogels could be clearly achieved, so that the cell adhesion could be specifically and precisely controlled. The sizes and distances of the line or rectangular patterns could be further specifically varied for any kinds of applications by tuning of the stamp sizes during the wet µ-CdP process, underlining the versatility of this technique. It is important to note again that no bio-functionalization was required for the effective cell adhesion. Probably, cell adhesion-mediating molecules,

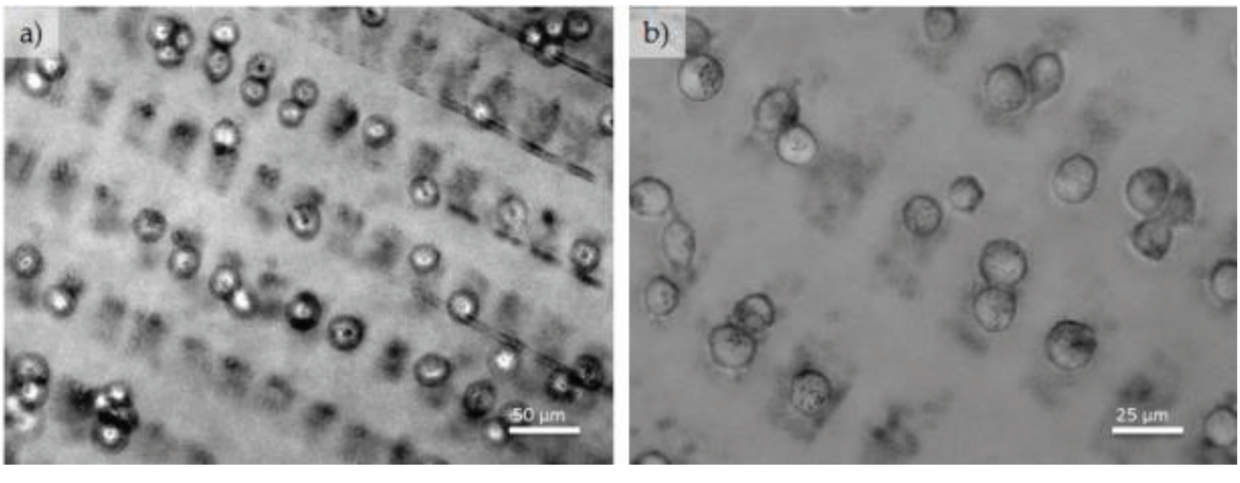

Figure 13. (a–b) Optical images of fibroblast adhesion on an Au NPs-patterned PEG hydrogel exhibiting rectangular patterns of Au NPs. Scale bars: (a) 50 µm; (b) 25 µm [12].

for example, proteins such as fibronectin and vinculin, bind (non-specifically) to the surface of the Au NPs, thereby replacing the citrate molecules. Our observation that without proteins in the medium (serum-free medium), no cell adhesion could be observed supports this assumption. While these well-defined μ-patterns of Au NPs have proven to be very useful to control cell adhesion at predefined areas, for other applications of Au NPs patterns such as in nano-plasmonics and -photonics, nanoscale pattern dimensions are also highly desirable.

2.4.3. Nano-contact transfer via wrinkled PDMS stamps

A simple, yet very effective method to make nano-patterns of Au NPs was invented by Whitesides and perfected by Fery [60, 69]. It takes advantage of the wrinkling that occurs at the surface of an elastomer exhibiting a thin, hard skin, which can be created by plasma treatment of a slab of the elastomer in a stretched conformation, upon relaxation to the original size [60]. We made use of this great invention and modified the PDMS stamp's surface and employed the nano-sized wrinkles for nano-sized patterning of Au NPs on PEG hydrogels by stamping [61].

First of all, wrinkled PDMS stamps were prepared via plasma oxidation of smooth PDMS molds in a stretched configuration and subsequent relaxation of the stamp to the original macroscopic dimensions (see **Figure 14**) [60]. By this wrinkling process, periodic and regular nano-line topographies were achieved on the surface of the PDMS stamps. The characteristic lateral and vertical dimensions appeared to depend in a predictable way on the plasma treatment time and energy. In this case, the distances of the nano-lines (from hill to hill) varied from around 0.3 μm up to around 0.6 μm by choosing a plasma oxidation time of 2 up to 15 min, respectively. Generally, it can be said that the longer the plasma oxidation time, the wider the distances of the line spaces and the deeper the grooves were [61].

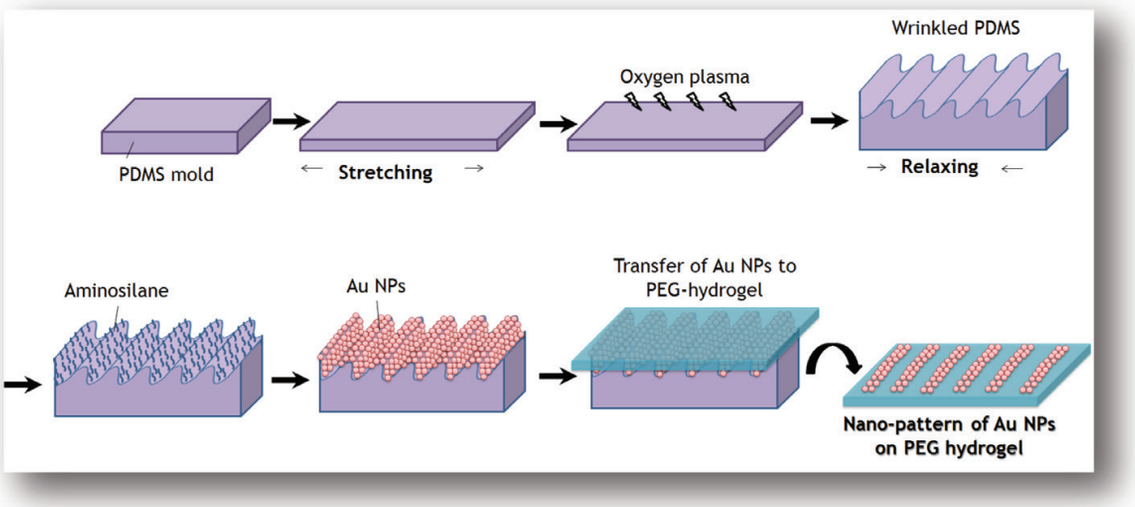

Figure 14. Schematic view of the nano-patterning of Au NPs on PEG hydrogel using wrinkled PDMS stamps [60].

In the next step, the surfaces of the wrinkled PDMS stamps were silanized with amino-silanes. The amino-silanized surfaces were subsequently coated with Au NPs. Coating of the PDMS stamp with amino-silane layer was crucial for having a good coverage of Au NPs interacting with the surface via electrostatic interactions, and which could be easily transferred to the desired end surfaces. Without amino-silane layer, no Au NPs could be seen on the PDMS stamp.

After an Au NPs-coated PDMS stamp was obtained, the Au NPs were transferred via stamping onto PEG hydrogels and cell adhesion on the nano-patterned Au NPs on PEG hydrogels were investigated. As seen in **Figure 15(a)**, the cells were adhering effectively on the nano-patterned surface containing Au NPs adhesion sites. The nano-pattern, which was transferred on PEG hydrogel, is shown in **Figure 15(b)** and **(c)** via AFM 2D and 3D height images and a cross-sectional profile.

As is already obvious from the optical micrograph in **Figure 15(a)** and is further recognized in **Figure 16(a)**, the fibroblasts do adhere quite clearly, but protrude and spread in random directions.

Part labels (b) and (c) of **Figure 16** are the enlarged images of (a) where the focal adhesions and protrusions were more clearly visible. This can be easily understood when realizing that the dimensions of the adhesive nano-patterns and the micrometer-sized cells differ by at least one order of magnitude. In other words, the adherent cells are likely spanning over a large number of nano-lines, and any elongation or alignment is not translated to the overall cell morphology.

Besides being able to direct specific cell adhesion on these nano-patterns of Au NPs on PEG-based hydrogels, these nano-patterned hydrogels can also serve as a very useful platform to immobilize certain bio-functional molecules, such as proteins, enzymes, antibodies, or supramolecular building blocks with great precision. Consequently, advanced applications

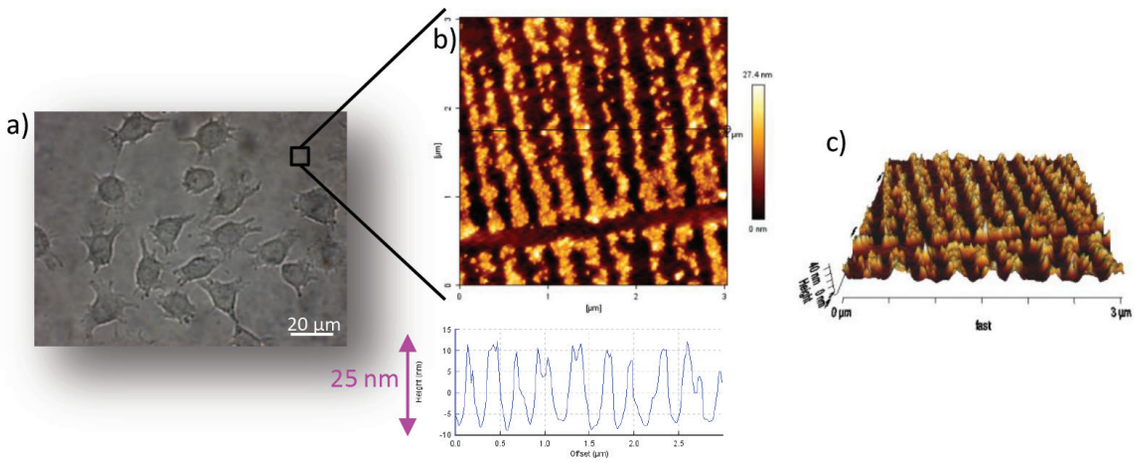

Figure 15. (a) Optical micrographs of cell adhesion on nano-patterned PEG hydrogel, fixed via formaldehyde; (b) AFM 2D height images and cross-sectional profile and (c) AFM 3D height images of Au NPs nano-lines on the surface of PEG hydrogel done with wrinkled PDMS Stamps. Scale bars: (a) 20 µm; (b) 500 nm. Images modified from Bowden et al. [60].

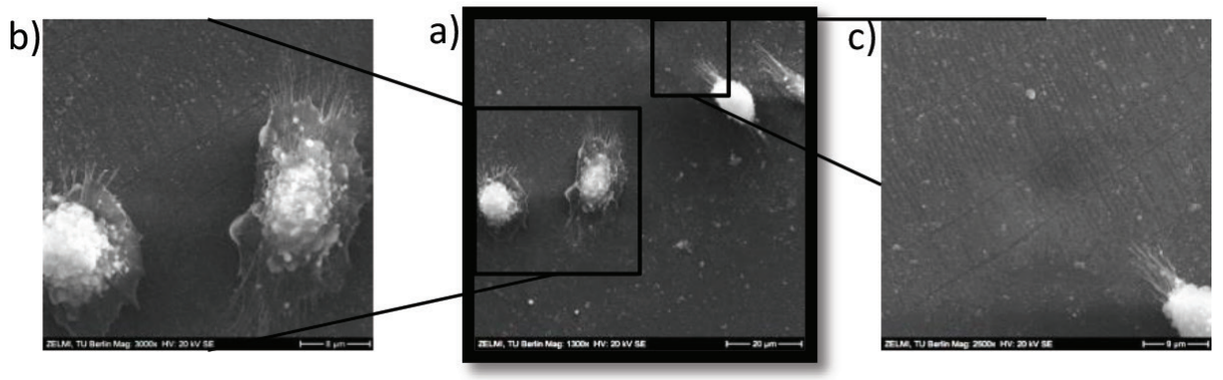

Figure 16. (a–c) SEM images of cell adhesion on Au NPs nano-patterns on PEG hydrogel. Scale bars: (a) 20 μm; (b) 8 μm; (c) 9 μm.

in biosensors and diagnostics are conceivable. Of particular interest are the modern readout methods that exploit surface plasmon resonance and surface-enhanced Raman effects, relying on relatively small probe molecules or possibly even whole cells.

3. Conclusions

Gold nanoparticles (Au NPs) with different sizes and shapes were synthesized and patterned on PEG-based hydrogels using different novel patterning strategies. Hereby, PEG hydrogels with different elastic or chemical properties could be synthesized depending on (i) the molecular structure of the macromonomer precursors (i.e., linear PEG or eight-arm star-shaped PEG), (ii) the crosslinking mechanism (e.g., UV-photopolymerization or Michael-type addition reactions), and by exploiting creating chemically modified hydrogel films with reactive end groups. The pattern sizes of Au NPs on the PEG hydrogels could be varied from the nanoscale to the microscale and with lines or rectangular pattern shapes.

On these Au NPs, cell culture studies were carried out and the results show that the cells only and effectively adhered on those areas where Au NPs were present, while the areas of pure, non-functional PEG hydrogels were free of cells. It is interesting to note that, using our presented unique nano- and micro-patterning strategies, neither for the transfer process of the Au NPs onto PEG hydrogels nor for the cell adhesion, any specific linkers or specific biofunctionalization with cell adhesion molecules were required for achieving the clearly selective eventual cell adhesion.

Besides their demonstrated applicability to control selective, localized adhesion of tissue cells, which was the focus of this chapter, and the Au NPs, which were synthesized with different sizes and shapes, exhibit different specific plasmon absorptions in the visible- or even near-infrared (NIR) range. This offers the possibility of employing these nanocomposite biomaterials (i.e., tailor-made Au NPs on tunable PEG hydrogels) to be applied in biosensor devices, for example, using SERS or (L)SPR phenomena as well. Finally, they are

promising nanomaterials for various other biomedical applications, for example, photothermal therapy, which can, for example, be used for cancer treatments or for controlled drug delivery and release.

Author details

Cigdem Yesildag, Zhenfang Zhang, Fang Ren, Gonzalo de Vicente and Marga C. Lensen*

*Address all correspondence to: lensen@chem.tu-berlin.de

Technische Universität Berlin, Nanopatterned Biomaterials, Berlin, Germany

References

[1] Faraday M. The Bakerian lecture: Experimental relations of gold (and other metals) to light. Philosophical Transactions of the Royal Society of London. 1857;**147**(January): 145-181

[2] Saha K, Agasti SS, Kim C, Li X, Rotello VM. Gold nanoparticles in chemical and biological sensing. Chemical Reviews. 2012;**112**(5):2739-2779

[3] Daniel MC, Astruc D. Gold nanoparticles: Assembly, supramolecular chemistry, quantum-size-related properties, and applications toward biology, catalysis, and nanotechnology. Chemical Reviews. 2004;**104**:293-346

[4] Giljohann DA, Seferos DS, Daniel WL, Massich MD, Patel PC, Mirkin CA. Gold nanoparticles for biology and medicine. Angewandte Chemie (International Ed. in English). Apr 2010;**49**(19):3280-3294

[5] Yu Y, Chang S, Lee C, Wang CRC. Gold Nanorods: Electrochemical synthesis and optical properties. Journal of Physical Chemistry B. 1997;**101**(34):6661-6664

[6] Alkilany AM, Thompson LB, Boulos SP, Sisco PN, Murphy CJ. Gold nanorods: Their potential for photothermal therapeutics and drug delivery, tempered by the complexity of their biological interactions. Advanced Drug Delivery Reviews. 2012;**64**:190-199

[7] Ren F. Synthesis of Gold Nanoparticle-Hydrogel Nanocomposites with Controlled Cytotoxicity and Unique Cell-Adhesive Properties. Doctoral Thesis (Dissertatation). Berlin, Germany: Technische Universität Berlin in Berlin; 2016. http://dx.doi.org/10.14279/depositonce-5575

[8] Alkilany AM, Murphy CJ. Toxicity and cellular uptake of gold nanoparticles: What we have learned so far? Journal of Nanoparticle Research. Sep 2010;**12**(7):2313-2333

[9] Riley RS, Day ES. Gold nanoparticle-mediated photothermal therapy: Applications and opportunities for multimodal cancer treatment. WIREs Nanomed Nanobiotechnol. 2017;**9**:1-16

[10] Ren F, Yesildag C, Zhang Z, Lensen MC. Functional PEG-hydrogels convey gold nanoparticles from silicon and aid cell adhesion onto the nanocomposites. Chemistry of Materials. 2017;**29**:2008-2015

[11] Ren F, Yesildag C, Zhang Z, Lensen M. Surface patterning of gold nanoparticles on PEG-based hydrogels to control cell adhesion. Polymers (Basel). Apr 2017;**9**(5):154

[12] Yesildag C, Bartsch C, de Vicente G, Lensen M. Novel wet micro-contact deprinting method for patterning gold nanoparticles on PEG-hydrogels and thereby controlling cell adhesion. Polymers (Basel). May 2017;**9**(5):176

[13] Williams DF. Definitions in biomaterials. In: Proceedings of a Consensus Conference of the European Society for Biomaterials. Vol. 4. New York: Elsevier; 1987

[14] Saini M, Singh Y, Arora P, Jain K. Implant biomaterials: A comprehensive review. World Journal of Clinical Cases. 2015;**3**(1):52-57

[15] Davis JR. Overview of biomaterials and their use in medical devices. In: Davis JR, editor. Handbook of Materials for Medical Devices. Ohio: ASM International; 2003. pp. 1-12

[16] Lee KY, Mooney DJ. Hydrogels for tissue engineering. Chemical Reviews. 2001;**101**(7): 1869-1880

[17] El-Sherbiny IM, Yacoub MH. Hydrogel scaffolds for tissue engineering: Progress and challenges. Global Cardiology Science and Practice. 2013;**2013**(3):316-342. DOI: 10.5339/gcsp.2013.38

[18] Seal BL, Otero TC, Panitch A. Polymeric biomaterials for tissue and organ regeneration. Materials Science and Engineering R. 2001;**34**:147-230

[19] Vo-Dinh T, Cullum B. Biosensors and biochips: Advances in biological and medical diagnostics. Fresenius Journal of Analytical Chemistry. 2008;**366**(6):540-551

[20] Veitinger M, Oehler R, Umlauf E, Baumgartner R, Schmidt G, Gerner C, Babeluk R, Attems J, Mitulovic G, Rappold E, Lamont J, Zellner M. A platelet protein biochip rapidly detects an Alzheimer ' s disease – specific phenotype. Acta Neuropathologica. 2014;**128**(5): 665-677

[21] Ferrari M, Bashir R, Wereley S. Volume IV: Biomolecular sensing, processing and analysis. In: Ferrari M, Bashir R, Wereley S, editors. BioMEMS and Biomedical Nanotechnology. 410. US: Springer; 2007. p. XXII

[22] Shruthi GS, Amitha CV, Mathew BB. Biosensors: A modern day achievement, Journal of Instumentation Technology. 2014;**2**(1):26-39

[23] Lee TM. Over-the-counter biosensors: Past, present, and future. Sensors. 2008;**8**:5535-5559

[24] Sabr AK. Biosensors. American Journal of Biomedical Engineering. 2016;**6**(6):170-179

[25] Wichterle O, Lim D. Hydrophilic gels for biological use. Nature. 1960;**185**(4706):117-118

[26] Jen AC, Wake MC, Mikos AG. Review: Hydrogels for cell immobilization. Biotechnology and Bioengineering. 1996;**50**:357-364

[27] Park JB, Lakes RS. Biomaterials: An Introduction. 3rd ed. New York: Springer; 2007

[28] Patel NR, Gohil PP. A review on biomaterials: Scope, applications & human anatomy significance. International Journal of Emerging Technology and Advanced Engineering. 2012;**2**(4):91-101

[29] Gorbet MB, Sefton MV. Biomaterial-associated thrombosis: Roles of coagulation factors, complement, platelets and leukocytes. Biomaterials. 2004;**25**:5681-5703

[30] Brien FJO. Biomaterials & scaffolds for tissue engineering. Materials Today. 2011;**14**(3):88-95

[31] Zalipsky S, Harris JM. Poly(ethylene glycol) Chemistry and Biological Applications. ACS Symposium Series. 1997;**680**(2):1-13. ISBN13: 9780841235373e, ISBN: 9780841216440. DOI: 10.1021/bk-1997-0680.ch001

[32] Lensen MC, Schulte VA, Diez M. Cell adhesion and spreading on an intrinsically anti-adhesive PEG biomaterial. In: Pignatello PR, editor. Biomaterials – Physics and Chemistry. Rijeka, Croatia: InTech; 2011. pp. 397-414

[33] Schulte VA, Diez M, Möller M, Lensen MC. Surface topography induces fibroblast adhesion on intrinsically nonadhesive poly (ethylene glycol) substrates. Biomacromolecules. 2009;**10**:2795-2801

[34] Diez M, Schulte VA, Stefanoni F, Natale CF, Mollica F, Cesa CM, Chen J, Möller M, Netti PA, Ventre M, Lensen MC. Molding micropatterns of elasticity on PEG-based hydrogels to control cell adhesion and migration. Advanced Engineering Materials. Oct 2011;**13**(XX):16-18

[35] Kelleher SM, Zhang Z, Löbus A, Strehmel C, Lensen MC. Blending PEG-based polymers and their use in surface micro-patterning by the FIMIC method to obtain topographically smooth patterns of elasticity. Biomaterials Science. 2014;**2**(3):410-418

[36] de Vicente G, Lensen MC. Topographically and elastically micropatterned PEG-based hydrogels to control cell adhesion and migration. European Polymer Journal. 2016;**78**:290-301

[37] Strehmel C, Perez-Hernandez H, Zhang Z, Löbus A, Lasagni AF, Lensen MC. Geometric control of cell alignment and spreading within the confinement of Antiadhesive poly(ethylene glycol) microstructures on laser-patterned surfaces. ACS Biomaterials Science & Engineering. 2015;**1**(9):747-752

[38] Chen CS, Mrksich M, Huang S, Whitesides GM, Ingber DE. Geometric control of cell life and death. Science (80–). 1997;**276**(5317):1425-1428

[39] Chen CS, Mrksich M, Huang S, Whitesides GM, Ingber DE. Micropatterned surfaces for control of cell shape, position, and function. Biotechnology Progress. 1998;**7938**(98): 356-363

[40] Wang X, Li S, Yan C, Liu P, Ding J. Fabrication of RGD micro/nanopattern and corresponding study of stem cell differentiation. Nano Letters. 2015;**15**(3):1457-1467

[41] Glass R, Möller M, Spatz JP. Block copolymer micelle nanolithography. Nanotechnology. 2003;**14**(10):1153-1160

[42] Arnold M, Cavalcanti-Adam EA, Glass R, Blümmel J, Eck W, Kantlehner M, Kessler H, Spatz JP. Activation of integrin function by nanopatterned adhesive interfaces. Chemphyschem. Mar 2004;**5**(3):383-388

[43] Graeter SV, Huang J, Perschmann N, López-García M, Kessler H, Ding J, Spatz JP. Mimicking cellular environments by nanostructured soft interfaces. Nano Letters. May 2007;**7**(5):1413-1418

[44] Young JL, Holle AW, Spatz JP. Nanoscale and mechanical properties of the physiological cell-ECM microenvironment. Experimental Cell Research. 2016;**343**(1):3-6

[45] Guasch J, Diemer J, Riahinezhad H, Neubauer S, Kessler H, Spatz JP. Synthesis of binary nanopatterns on hydrogels for initiating cellular responses. Chemistry of Materials. 2016; **28**(6):1806-1815

[46] de Vicente G. Controlled Migration of Cells on Mechanically, Physically and Chemically Patterned Biomaterials. Doctoral Thesis (Dissertatation). Berlin, Germany: Technische Universität Berlin; 2015. urn:nbn:de:kobv:83-opus4-64976, http://dx.doi.org/10.14279/depositonce-4404

[47] Heuberger A. X-ray lithography. Journal of Vacuum Science & Technology B: Microelectronics and Nanometer Structures Processing, Measurement, and Phenomena. Jan 1988;**6**(1):107

[48] Pease RFW. Electron beam lithography. Contemporary Physics. 1981;**22**(3):265-290

[49] Vieu C, Carcenac F, Pépin A, Chen Y, Mejias M, Lebib A, Manin-Ferlazzo L, Couraud L, Launois H. Electron beam lithography: Resolution limits and applications. Applied Surface Science. 2000;**164**(1):111-117. DOI: 10.1016/S0169-4332(00)00352-4

[50] Wouters D, Schubert US. Nanolithography and nanochemistry: Probe-related patterning techniques and chemical modification for nanometer-sized devices. Angewandte Chemie (International Ed. in English). 2004;**43**(19):2480-2495

[51] Piner RD, Zhu J, Xu F, Hong S, Mirkin CA. 'Dip-pen' nanolithography. Science (80–). 1999;**283**(5402):661-663

[52] Kumar A, Whitesides GM. Features of gold having micrometer to centimeter dimensions can be formed through a combination of stamping with an elastomeric stamp and an alkanethiol 'ink' followed by chemical etching. Applied Physics Letters. 1993; **63**(14):2002-2004

[53] Tien J, Xia Y, Whitesides GM. Microcontact printing of SAMs. Thin Film. 1998;**24**: 227-250

[54] Kelleher S, Jongerius A, Loebus A, Strehmel C, Zhang Z, Lensen MC. AFM Characterization of elastically micropatterned surfaces fabricated by fill-molding in capillaries (FIMIC) and investigation of the topographical influence on cell adhesion to the patterns. Advanced Engineering Materials. Mar. 2012;**14**(3):56-66

[55] Chen J, Mela P, Möller M, Lensen MC. Microcontact deprinting: A technique to pattern gold nanoparticles. ACS Nano. 2009;**3**(6):1451-1456

[56] Díez M, Mela P, Seshan V, Möller M, Lensen MC. Nanomolding of PEG-based hydrogels with sub-10-nm resolution. Small. 2009;**5**(23):2756-2760

[57] Chen J, Arafeh M, Guiet A, Felkel D, Loebus A, Kelleher SM, Fischer A, Lensen MC. Hybrid hierarchical patterns of gold nanoparticles and poly(ethylene glycol) microstructures. Journal of Materials Chemistry C. 2013;**1**(46):7709-7715

[58] Kim E, Xia Y, Whitesides GM. Micromolding in capillaries: Applications in materials science. Journal of the American Chemical Society. Jan 1996;**118**(24):5722-5731

[59] Xia Y, Kim E, Whitesides GM. Micromolding of polymers in capillaries: Applications in microfabrication. Chemistry of Materials. Jan 1996;**8**(7):1558-1567

[60] Bowden N, Huck WTS, Paul KE, Whitesides GM. The controlled formation of ordered, sinusoidal structures by plasma oxidation of an elastomeric polymer. Applied Physics Letters. 1999;**75**(17):2557

[61] Yesildag C, Tyushina A, Lensen M. Nano-contact transfer with gold nanoparticles on PEG Hydrogels and using wrinkled PDMS-stamps. Polymers. 2017;**9**(6):199

[62] Bastús NG, Comenge J, Puntes V. Kinetically controlled seeded growth synthesis of citrate-stabilized gold nanoparticles of up to 200 nm: Size focusing versus Ostwald ripening. Langmuir. Sep 2011;**27**(17):11098-11105

[63] Wang W, Pang Y, Yan J, Wang G, Suo H, Zhao C, Xing S. Facile synthesis of hollow urchin-like gold nanoparticles and their catalytic activity. Gold Bulletin. Jun 2012;**45**(2):91-98

[64] Fiévet F, Lagier JP, Figlarz M. Preparing monodisperse metal powders in micrometer and submicrometer sizes by the polyol process. Materials Research Society Bulletin. 1989;**14**:29-32

[65] Ye X, Jin L, Caglayan H, Chen J, Xing G, Zheng C, Doan-Nguyen V, Kang Y, Engheta N, Kagan CR, Murray CB. Improved size-tunable synthesis of monodisperse gold nanorods through the use of aromatic additives. ACS Nano. Mar 2012;**6**(3):2804-2817

[66] Zhang Z, Loebus A, de Vicente G, Ren F, Arafeh M, Ouyang Z, Lensen MC. Synthesis of poly(ethylene glycol)-based hydrogels via amine-Michael type addition with tunable stiffness and postgelation chemical functionality. Chemistry of Materials. Jun 2014; **26**(12):3624-3630

[67] Strehmel C. Zelluläre Reaktionen Muriner Fibroblasten Auf Planaren Und Strukturierten Polyethylenglykol-Basierten Biomaterialien. Doctoral Thesis (Dissertatation). Berlin, Germany: Technische Universität Berlin; 2013. https://depositonce.tu-berlin.de/bitstream/11303/5636/1/c3bm60055f.pdf

[68] Li H, Zhang J, Zhou X, Lu G, Yin Z, Li G, Wu T, Boey F, Venkatraman SS, Zhang H. Aminosilane micropatterns on hydroxyl-terminated substrates: Fabrication and applications. Langmuir. Apr 2010;**26**(8):5603-5609

[69] Pazos-Pérez N, Ni W, Schweikart A, Alvarez-Puebla RA, Fery A, Liz-Marzán LM. Highly uniform SERS substrates formed by wrinkle-confined drying of gold colloids. Chemical Science. 2010;**1**(2):174